

## **On the controversy of metal ion composition on Amine oxygenase (AurF): A computational investigation**

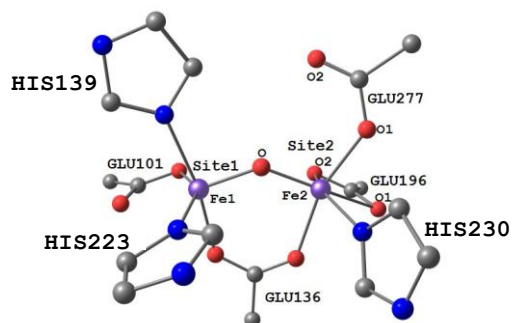
**Prabha Jaypal\* and Gopalan Rajaraman\***

*Department of chemistry, Indian Institute of Technology-Bombay, Powai, Mumbai. Fax: +91-22-2572-3480; Tel: +91-22-2576-7183; E-mail: [rajaraman@gmail.com](mailto:rajaraman@gmail.com), [prabha.jaypal@gmail.com](mailto:prabha.jaypal@gmail.com)*

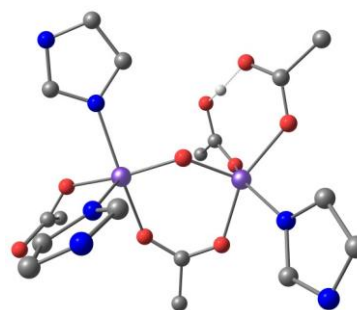
## Electronic Supplementary Information (ESI):

Figure S1: B3LYP optimized geometries of the models investigated in this paper. The hydrogen atoms (except those involved in H-bonding) are omitted for clarity.

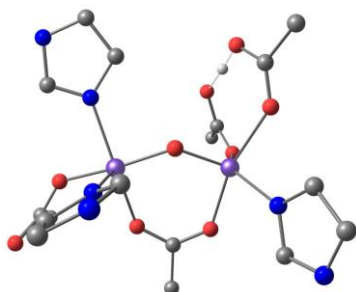
**M1- Fe<sup>III</sup>,Fe<sup>III</sup>,Oxo, (M1)**



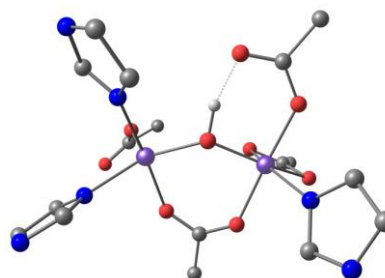
**<sup>196</sup>M1- Fe<sup>III</sup>,Fe<sup>III</sup>, Oxo, Glutamate 196 protonated.**



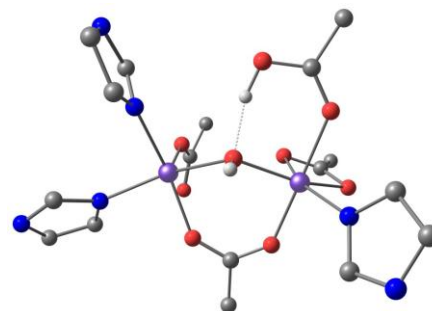
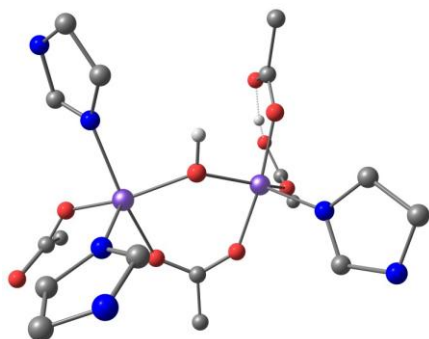
**<sup>277</sup>M1-Fe<sup>III</sup>, Fe<sup>III</sup>, Oxo, Glutamate 277 protonated.**



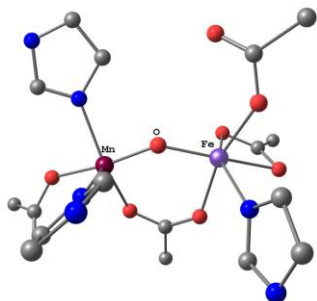
**M1P- Fe<sup>III</sup>, Fe<sup>III</sup>, Hydroxo**



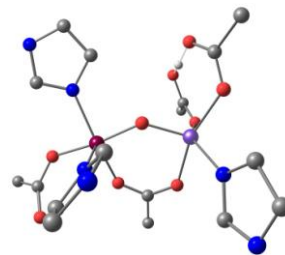
**<sup>196</sup>M1P- Fe<sup>III</sup>, Fe<sup>III</sup>, Hydroxo, Glutamate 196 protonated.** **<sup>277</sup>M1P- Fe<sup>III</sup>, Fe<sup>III</sup>, Hydroxo, Glutamate 277 protonated.**



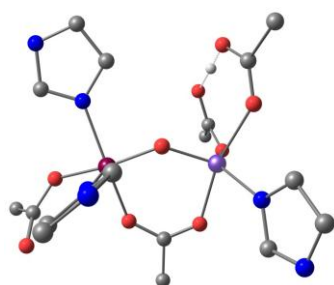
**M2- Mn<sup>III</sup>,Fe<sup>III</sup>, Oxo**



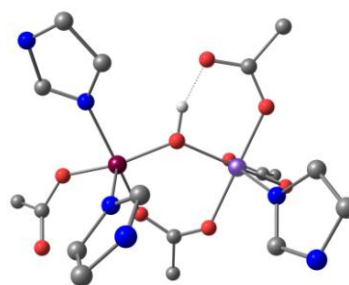
**<sup>196</sup>M2- Mn<sup>III</sup>,Fe<sup>III</sup>, Oxo, Glutamate 196 protonated.**



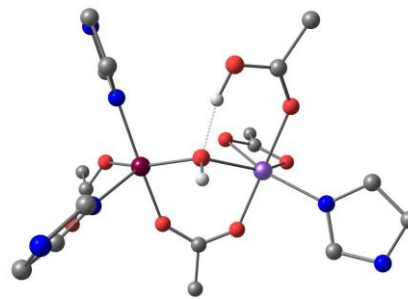
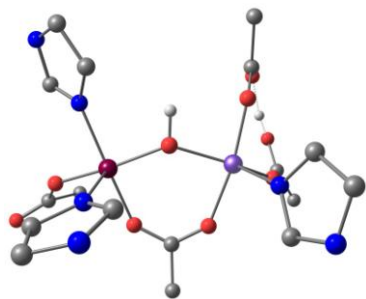
**<sup>277</sup>M2- Mn<sup>III</sup>,Fe<sup>III</sup>, Oxo, Glutamate 277 protonated.**



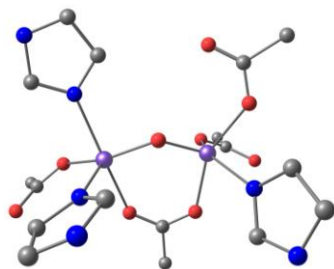
**M2P-Mn<sup>III</sup>, Fe<sup>III</sup>, Hydroxo.**



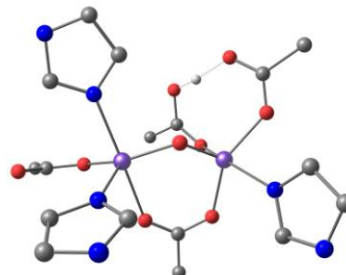
**<sup>196</sup>M2P-Mn<sup>III</sup>, Fe<sup>III</sup>, Hydroxo, Glutamate 196 protonated.** **<sup>277</sup>M2P- Mn<sup>III</sup>, Fe<sup>III</sup>, Hydroxo, Glutamate 277 protonated.**



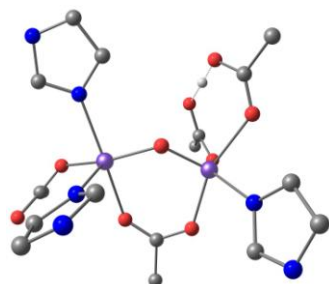
**M3- Fe<sup>II</sup>,Fe<sup>III</sup>,Oxo.**



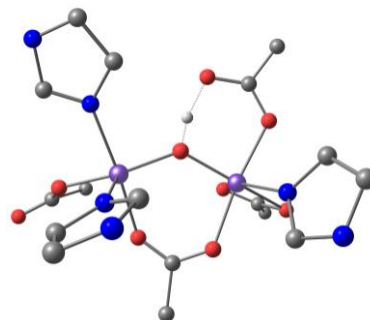
**<sup>196</sup>M3- Fe<sup>II</sup>,Fe<sup>III</sup>, Oxo, Glutamate 196 protonated**



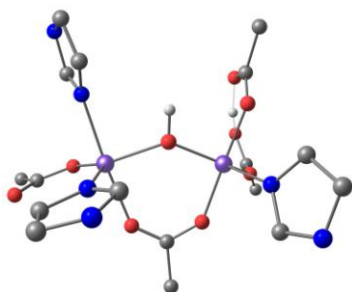
$^{277}\text{M3P-Fe}^{\text{II}}, \text{Fe}^{\text{III}}, \text{Oxo}, \text{Glutamate } 277 \text{ protonated}$



$\text{M3P-Fe}^{\text{II}}, \text{Fe}^{\text{III}}, \text{Hydroxo}$



$^{196}\text{M3P-Fe}^{\text{II}}, \text{Fe}^{\text{III}}, \text{Hydroxo}, \text{Glutamate } 196 \text{ protonate}$



$^{277}\text{M3P-Fe}^{\text{II}}, \text{Fe}^{\text{III}}, \text{Hydroxo}, \text{Glutamate } 277 \text{ protonated}$

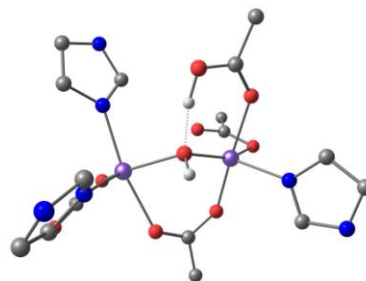
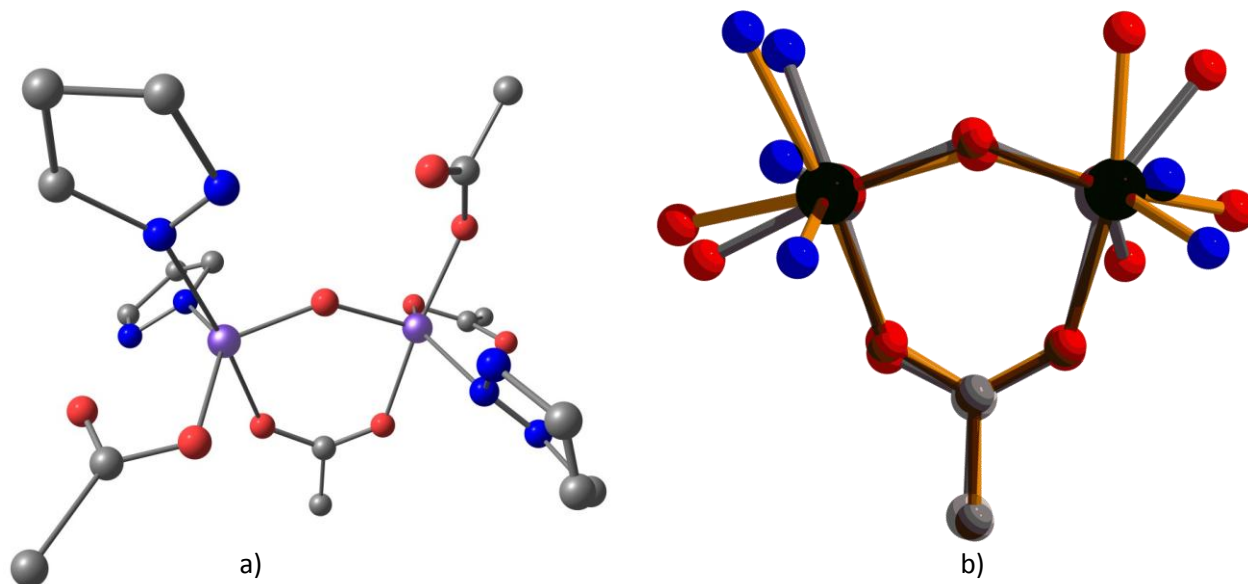


Figure S2: Synthetic model complex containing  $(\mu\text{-oxo})(\mu\text{-carboxylato})\text{diiron(III)}$  core<sup>1</sup> (phenyl ring were omitted for clarity) b) Superimposed structure of x-ray (structure with orange colour bond) and  $^{196}\text{MI}$  (structure with grey colour bond).



The popular B3LYP functional<sup>2</sup> in conjunction with TZVP basis set for Fe, Mn and SVP basis

set for rest of the elements are used for optimisation. The structure optimisation has been carried out in solution phase (water) to reliably predict the spectroscopic parameters. All initial coordinates are obtained from the X-ray crystal structure of the oxidized AurF enzyme<sup>3</sup> (PDB code: 3CHU). An unrestricted DFT (UDFT) methodology is used to model the spin polarization efficiently for open shell orbitals of both irons and manganese. This method enables the modelling of antiferromagnetic (AF) coupling between the two Fe atoms or between Mn-Fe by the use of a broken symmetry (BS) wave function. Geometry optimization is carried out with Gaussian 09 software,<sup>4</sup> whereas all spectroscopic parameters are calculated with the ORCA 2.8 program package.<sup>5</sup> The best suitable functional have been chosen based on the property of interest as reported earlier.<sup>6, 7</sup> Since the prediction of these parameters requires a reasonable estimation of spin densities on the metal centres, the employed exchange-correlations functional play a crucial role in computing these parameters. The NSP, EPR and Mössbauer parameters were calculated using BP86 functional and TZVP basis set.<sup>6</sup> However the UV spectral calculation and the Heisenberg coupling constant  $J$  were obtained by employing B3LYP functional and TZVP basis set.<sup>7</sup> The Mössbauer isomer shifts  $\delta$  are calculated based on  $\rho(0)$ :

$$\delta = a (\rho(0) - A) + C \quad \text{Eq.1}$$

where, a and b are constant and  $\rho(0)$  is the electron density at the nucleus.

Table S1: B3LYP optimized bond lengths (Å) of the oxidized models with di-iron metal center.

Bond length	<i>MI</i>	<i><sup>196</sup>MI</i>	<i><sup>277</sup>MI</i>	<i>MIP</i>	<i><sup>196</sup>MIP</i>	<i><sup>277</sup>MIP</i>	X-ray <sup>3</sup>
Fe1 <sup>a</sup> -Fe2 <sup>b</sup>	3.355	3.325	3.341	3.566	3.659	3.627	3.503
Fe1- $\mu$ O	1.794	1.825	1.827	1.928	1.933	2.070	1.942
Fe2- $\mu$ O	1.805	1.774	1.776	1.953	1.981	2.050	1.986
Fe1-O <sub>1</sub> GLU101	1.970	1.941	1.949	1.865	1.875	1.849	2.056
Fe1-O <sub>2</sub> GLU101	3.890	3.500	3.755	3.572	3.694	3.380	4.148
Fe1-N His139	2.167	2.142	2.145	2.146	2.130	2.118	2.312
Fe1-N His223	2.090	2.077	2.079	2.116	2.056	2.097	2.275
Fe2-O Glu227	1.994	2.006	2.121	1.986	1.948	2.099	1.908
Fe2-N His 230	2.172	2.136	2.136	2.118	2.047	2.080	2.148
Fe2-O1 GLU196	2.340	2.087	1.970	2.149	2.011	2.098	1.960
Fe2-O2 GLU196	2.089	3.538	3.416	2.136	3.624	2.107	2.716
Fe1-O Glu136 (brig)	2.086	2.076	2.064	2.021	2.031	2.016	2.018

Fe2-O Glu136(brig)	2.139	2.047	2.052	2.050	1.987	1.976	1.992
Fe1-O-Fe2	137	135	136	133	134	123	126

<sup>a</sup> site 1, <sup>b</sup> site 2

Table S2: B3lyp optimized bond lengths (Å) of the oxidized models with Manganese-iron metal center.

Bond length	<i>M2</i>	<i><sup>196</sup>M2</i>	<i><sup>277</sup>M2</i>	<i>M2P</i>	<i><sup>196</sup>M2P</i>	<i><sup>277</sup>M2P</i>	X-ray <sup>3</sup>
Mn1 <sup>a</sup> -Fe2 <sup>b</sup>	3.381	3.380	3.332	3.561	3.633	3.538	3.503
Mn1-μO	1.768	1.792	1.796	1.894	1.940	1.990	1.942
Fe2-μO	1.818	1.787	1.790	1.987	1.993	2.131	1.986
Mn1-O <sub>1</sub> GLU101	1.942	1.918	1.918	1.892	1.863	1.871	2.056
Mn1-O <sub>2</sub> GLU101	3.426	3.402	3.450	3.397	3.990	3.392	4.148
Mn1-N His139	2.193	2.090	2.086	2.062	2.044	2.051	2.312
Mn1-N His223	2.106	2.192	2.198	2.216	2.195	2.218	2.275
Fe2-O Glu227	1.991	2.008	2.111	1.978	1.935	2.061	1.908
Fe2-N His230	2.176	2.131	2.135	2.114	2.045	2.090	2.148
Fe2-O <sub>1</sub> GLU196	2.297	2.065	1.971	2.143	2.005	2.098	1.960
Fe2-O <sub>2</sub> GLU196	2.103	3.549	3.420	2.124	3.635	2.115	2.716
Fe1-O Glu136 (brig)	1.985	1.986	1.988	1.955	1.959	1.946	2.018
Fe2-O Glu136(brig)	2.154	2.063	2.057	2.047	1.992	1.982	1.992
Mn1-O-Fe2	141	138	136	133	135	118	126

<sup>a</sup> site 1, <sup>b</sup> site 2

Table S3: B3LYP optimized bond lengths (Å) of the mixed valent models with di-iron metal center.

Bond length	<i>M3</i>	<i><sup>196</sup>M3</i>	<i><sup>277</sup>M3</i>	<i>M3P</i>	<i><sup>196</sup>M3P</i>	<i><sup>277</sup>M3P</i>	X-ray <sup>3</sup>
Fe1 <sup>a</sup> -Fe2 <sup>b</sup>	3.297	3.288	3.321	3.603	3.683	3.532	3.503
Fe1-μO	1.878	1.899	1.901	2.025	2.065	2.170	1.942
Fe2-μO	1.762	1.752	1.751	1.914	1.912	2.009	1.986
Fe1-O <sub>1</sub> GLU101	2.036	2.049	2.023	2.016	2.002	1.981	2.056
Fe1-O <sub>2</sub> GLU101	4.194	3.379	3.631	3.200	3.061	3.305	4.148
Fe1-N His139	2.181	2.243	2.237	2.244	2.220	2.177	2.312
Fe1-N His223	2.262	2.168	2.177	2.168	2.153	2.151	2.275
Fe2-O Glu227	2.043	2.033	2.178	2.035	2.005	2.150	1.908

Fe2-N His230	2.217	2.181	2.166	2.155	2.080	2.106	2.148
Fe2-O1 GLU196	3.059	2.163	2.023	2.225	2.032	2.116	1.960
Fe2-O2 GLU196	2.035	3.586	3.398	2.113	3.611	2.134	2.716
Fe1-O Glu136 (brig)	2.234	2.255	2.214	2.199	2.180	2.220	2.018
Fe2-O Glu136(brig)	2.099	2.023	2.047	2.011	1.960	1.946	1.992
Fe1-O-Fe2	129	128	130	123	120	115	126

<sup>a</sup> site 1, <sup>b</sup> site 2

Table S4: Relative energy (kcal/mol) between the different protonated models at B3LYP level of theory.

models	<sup>196</sup> MI	<sup>277</sup> MI	<sup>196</sup> MIP	<sup>277</sup> MIP	<sup>196</sup> M2	<sup>277</sup> M2	<sup>196</sup> M2P	<sup>277</sup> M2P	<sup>196</sup> M3	<sup>277</sup> M3	<sup>196</sup> M3P	<sup>277</sup> M3P
Energy	0.079	0.0	0.00	1.141	0.076	0.0	0.0	3.593	0.0	2.600	0.0	0.061

Table S5:

Calculated and experimental <sup>8,9</sup> isomer shift  $\delta$  (mm/s), quadrupole splitting  $\Delta E_q$  (mm/s), g-tensor and Net spin Population (NSP) of oxidized model complexes investigated.

Oxidized state											
	<sup>196</sup> MI	<sup>277</sup> MI	<sup>196</sup> MIP	<sup>277</sup> MIP	<sup>196</sup> M2	<sup>277</sup> M2	<sup>196</sup> M2P	<sup>277</sup> M2P	<sup>196</sup> M3	<sup>277</sup> M3	Exp <sup>8,9</sup>
Net Spin Population											
NSP (Fe1/Mn1)	4.165	4.141	4.245	4.269	-3.801		-3.825	-3.912	-3.943		
NSP (Fe2)	-4.152	-4.169	-4.229	-4.247	4.169		4.155	4.245	4.260		
NSP( $\mu$ -O)	-0.032	0.119	-0.000	0.009	0.257		0.347	0.123	0.088		
Spectroscopic parameters											
g-tensor	-	-	-	-	2.028,2.052,2.075	2.029,2.055,2.083	2.036,2.042,2.066	2.036,2.050, 2.070	2.030,2.014,2.015		
Hyperfine Fe	-	-	-	-	-579.8,-614.7,-672.5	-554.0,-594.2,-640.2	-641.1,-675.0,-693.3	-615.4,-653.1,-675.1			
Hyperfine Mn	-	-	-	-	234.6, 410.0,689.5	196.0,430.2, 631.6	159.3,459.9, 528.0	163.3,483.2,500.9	210,270,322 (Mn)		
$\delta$ (Fe1/Mn1)	0.592	0.607	0.578	0.575	0.633	0.627	0.600	0.616	0.54		
$\delta$ (Fe2)	0.548	0.540	0.558	0.556	-	-	-	-	0.48		
$\Delta E_q$ (Fe1/Mn1)	-0.834	-0.890	-0.322	0.330	-2.628	2.579	-0.818	-1.749	0.80		
$\Delta E_q$ (Fe2)	-2.192	-1.793	-0.957	0.423	-	-	-	-	-1.86		

Table S6: Calculated and experimental <sup>9,10</sup> isomer shift  $\delta$  (mm/s), quadrupole splitting  $\Delta E_q$  (mm/s), g-tensor and Net spin Population (NSP) of the mixed valent state complexes investigated.

Mixed valence state					
	<i>M3</i>	<i><sup>277</sup>M3</i>	<i>M3P</i>	<i><sup>277</sup>M3P</i>	Exp <sup>9,10</sup>
Net Spin Population					
NSP (Fe1)	-3.708	-3.708	-3.789	-3.796	
NSP (Fe2)	4.098	4.073	4.238	4.250	
NSP( $\mu$ -O)	0.382	0.458	0.169	0.101	
Spectroscopic parameters					
g-tensor	1.90,1.94, 1.95	1.91, 1.94, 1.95	2.02,2.02,2.03	2.020, 2.02, 2.03	1.94,1.79,1.70
Hyperfine Fe1	-74,-77, -87	-65,-70,-82	-8,-9, -10	-7,-9, -10	
Hyperfine Fe2	19,72,76	25,77,80	-2,-8,-8	-3,-8, -8	
$\delta$ (Fe1)	0.619	0.979	0.901	0.871	1.24-Fe <sup>2+</sup>
$\delta$ (Fe2)	0.981	0.652	0.676	0.695	0.53-Fe <sup>3+</sup>
$\Delta E_q$ (Fe1)	1.371	2.132	1.807	1.813	+2.74-Fe <sup>2+</sup>
$\Delta E_q$ (Fe2)	1.791	-1.761	-0.412	0.917	-1.93-Fe <sup>3+</sup>

### **Computation of exchange interaction:**

The magnetic exchange interaction has been computed using the following spin-Hamiltonian.

$$H = -\sum_{i>j} J_{ij} \hat{S}_i \hat{S}_j$$

The magnetic exchange has been computed as the difference in energy between the high-spin state and the broken-symmetry state proposed by Noodleman.<sup>11</sup> There are many equations (spin-projected, non-spin projected)<sup>12</sup> advocated to compute the  $J$  values and here we are employing the methodology advocated by Ruiz and co-workers which has been shown to provide good numerical estimate of  $J$  values for numerous systems.

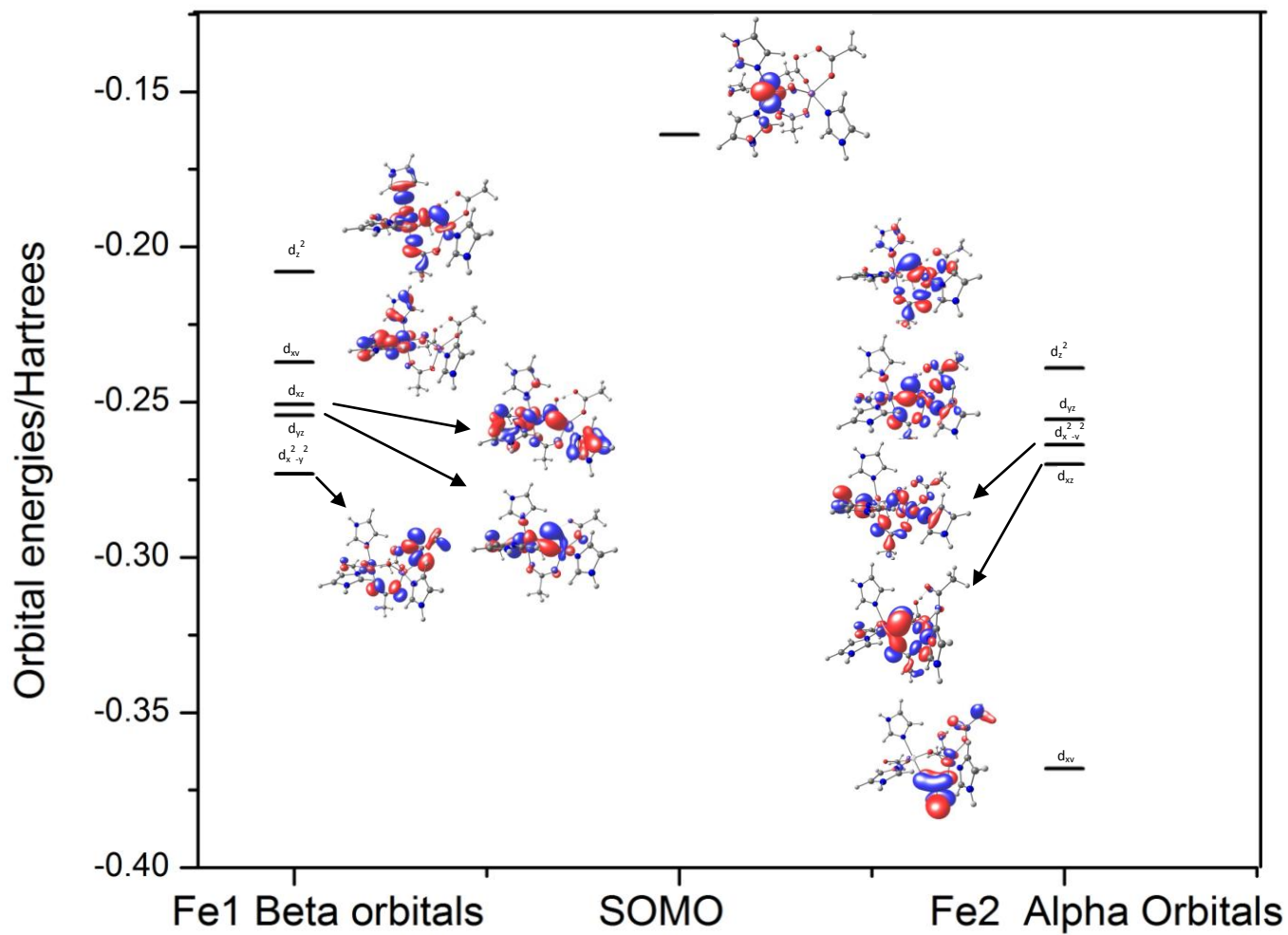


Table S7: Heisenberg coupling constant  $J$  ( $\text{cm}^{-1}$ ) computed at both B3LYP and BP86 functionals.

Models	B3LYP	BP86
M1	-185.6	-356.3
<sup>196</sup> M1	-194.6	-381.5
<sup>277</sup> M1	-188.1	-273.0
M1P	-47.2	-112.3
<sup>196</sup> M1P	-28.7	-70.2
<sup>277</sup> M1P	-12.8	-37.5
M2	-133.6	-258.2
<sup>196</sup> M2	-145.5	-276.6
<sup>277</sup> M2	-141.9	-268.5
M2P	-33.0	-70.1
<sup>196</sup> M2P	-24.6	-63.8
<sup>277</sup> M2P	-12.5	-27.0
M3	-200.7	-432.9
<sup>196</sup> M3	-198.1	-218.3
<sup>277</sup> M3	-*	-237.0
M3P	-42.8	-*
<sup>196</sup> M3P	-15.4	+121.2
<sup>277</sup> M3P	-16.8	-*

\* SCF convergence to BS solution was not successful.

Figure S3: Energies and the contour plot of the 3d orbitals for  $^{196}\text{M3}$  complex.



Reference:

1. S. Yoon and S. J. Lippard, *J. Am. Chem. Soc.*, 2004, **126**, 2666.
2. a) A. D. Becke, *J. Chem. Phys.*, 1993, **98**, 5648 b) A. D. Becke, *Phys. Rev. A: Gen. Phys.*, 1988, **38**, 3098.
3. Y. S. Choi, H. Zhang, J. S. Brunzelle, S. K. Nair and H. Zhao, *Proc. Natl. Acad. Sci.*, 2008, **105**, 6858.
4. M. J. Frisch, G. W. Trucks, H. B. Schlegel, G. E. Scuseria, M. A. Robb, J. R. Cheeseman, G. Scalmani, V. Barone, B. Mennucci, G. A. Petersson, H. Nakatsuji, M. Caricato, X. Li, H. P. Hratchian, A. F. Izmaylov, J. Bloino, G. Zheng, J. L. Sonnenberg, M. Hada, M. Ehara, K. Toyota, R. Fukuda, J. Hasegawa, M. Ishida, T. Nakajima, Y. Honda, O. Kitao, H. Nakai, T. Vreven, J. A. Montgomery, Jr., J. E. Peralta, F. Ogliaro, M. Bearpark, J. J. Heyd, E. Brothers, K. N. Kudin, V. N. Staroverov, R. Kobayashi, J. Normand, K. Raghavachari, A. Rendell, J. C. Burant, S. S. Iyengar, J. Tomasi, M. Cossi, N. Rega, J. M. Millam, M. Klene, J. E. Knox, J. B. Cross, V. Bakken, C. Adamo, J. Jaramillo, R. Gomperts, R. E. Stratmann, O. Yazyev, A. J. Austin, R. Cammi, C. Pomelli, J. W. Ochterski, R. L. Martin, K. Morokuma, V. G. Zakrzewski, G. A. Voth, P. Salvador, J. J. Dannenberg, S. Dapprich, A. D. Daniels, Ö. Farkas, J. B. Foresman, J. V. Ortiz, J. Cioslowski and D. J. Fox, *Gaussian, Inc.*, Wallingford CT, 2009.
5. F. Neese, *Comput. Mol. Sci.*, 2012, **2**, 73.
6. M. Römelt, S. Ye and F. Neese, *Inorg. Chem.*, 2009, **48**, 784.
7. P. Gasiorski, K. S. Danel, M. Matusiewicz, T. Uchacz, W. Kuźnik, Ł. Piątek and A. V. Kityk, *Mat. Chem. Phys.* 2012, **132**, 330
8. C. Krebs, L. Matthews Megan, W. Jiang and J. M. Bollinger, Jr., *Biochemistry* 2007, **46**, 10413-10418.
9. a) V. K. Korboukh, N. Li, E. W. Barr, J. M. Bollinger, Jr. and C. Krebs, *J. Am. Chem. Soc.*, 2009, 131, 13608 b) Y. S. Choi, H. Zhang, J. S. Brunzelle, S. K. Nair and H. Zhao, *Proc. Natl. Acad. Sci.*, 2008, **105**, 6858.
10. J. H. Rodriguez, H. N. Ok, Y. M. Xia, P. G. Debrunner, B. E. Hinrichs, T. Meyer and N. H. Packard, *J. Phys. Chem.* 1996, **100**, 6849.
11. L. Noodleman, *J. Chem. Phys.*, 1981, **74**, 5737.

12. A) E. Ruiz, S. Alvarez, A. Rodriguez-Forteza, P. Alemany, Y. Pouillon and C. Massobiro, *Magnetism: Molecules to Materials II*, edited by J. S. Miller and M. Drillon, 2001, 227.
- b) A. Bencini, F. Totti, C. A. Daul, K. Doclo, P. Fantucci and V. Barone, *Inorg. Chem.*, 1997, **36**, 5022.